GIS based allowable bearing capacity thematic maps of shallow foundation for Bogura District, Bangladesh

Md. Mahabub Rahman *1

1 Hajee Mohammad Danesh Science and Technology university, Department of Civil Engineering, Bangladesh, mmr.civil@hstu.ac.bd

Abstract

This investigation aims to create thematic maps of the allowable load-bearing capacity (BC) of shallow footings based on the findings of standard penetration tests (SPTs) carried out in Bogura District. Structural engineers utilize the allowable soil BC to calculate the required dimensions of the shallow footing for the buildings they want to build. 255 boreholes (BHs) were drilled in the research region, which were dispersed randomly. Four SPTs were conducted in each borehole at depths of 1.5, 3, 6, and 9 m, measured from the current ground level (EGL). To assess the accurate SPT-N values, a variety of criteria were taken into consideration, including the unit weight, the groundwater table (GWT), and other correction factors. The allowed soil BC at 1.5, 3, 6, and 9 meters was then estimated using the adjusted SPT-N values. The final product is a set of themed GIS maps of the city, each hue representing a different number for the permissible soil holding capacity. Since clay is present at shallow depths, the allowable BC in 86.5% of the region at 1.5 m depth was less than 73.13 kN/m², and in 82.4% of the area at 3 m depth, it was between 64.38 and 96.31 kN/m². For the whole area, the predicted permissible BC for depths of 6 and 9 meters was greater than 100 kN/m². Various local authorities can use these maps to determine the appropriate type of foundation and forecast the soil carrying capacity. It may also be used to evaluate the likelihood of failure and collapse as well as the foundations of both existing and poorly designed buildings.

1. Introduction

A subsurface study is required to get geotechnical characterizations to plan the foundation system for civil engineering constructions. The design of the lower structural component known as the substructure is greatly influenced by the geological characteristics of the subsurface soil [1-2]. The Standard Penetration Test (SPT) is a popular method for determining soils in situ subsurface characteristics. This test is often used in Bangladesh for various kinds of soil. This test was first offered by the Raymond Pile Company in 1902, and it is still the most widely used in situ test in the world today [3]. ASTM D 1586 [4] and AASHTO T-206 [5] provide specific instructions on how to perform the SPT. Researchers suggest that the test's findings can reliably predict soil geotechnical characteristics like compressibility, shear strength, and density. SPT results are accepted for the initial design of foundations due to its ease of use, affordability, and wide availability of SPT equipment [6-8]. The measured N values need to be

adjusted in several distinct ways before they can be used to estimate and compute soil geotechnical characteristics. It is important to consider the adjusted N-value to obtain more trustworthy findings. Based on their findings, many studies have suggested adopting these corrections to remove measurement N-value uncertainty; nonetheless, choosing the appropriate changes is essential to avoiding the need for further field measurements or lab computations [9-10].

Bearing capacity is a generic word that refers to a foundation soil's ability to withstand and transfer loads from a building. The typical foundation design is based on the principle of bearing capacity, often known as allowed bearing pressure. For preliminary design, the findings of SPTs may be utilized to assess the permissible bearing capacity of soil [11-13]. Before evaluating the allowable bearing capacity of soil, it is essential to correct the SPT value in order to achieve a more precise outcome. GIS is a valuable tool in engineering that can combine coordinate-based data with values for visual representation. GIS uses interpolation techniques

effectively to produce geotechnical maps with spatial distributions. GIS has been utilized in civil engineering for various purposes like earthquake damage assessment [14], various risk assessment [15], mapping soil types [16], mapping SPT-N values and bearing capacities [17], road mapping [18], soil loss assessment [19], water resource assessment [20], Land use land cover change [21-22]. In 2025, Hossain and Rahman utilized the IDW interpolation technique based on GIS to develop a seismic zonation map called a modified Mercalli intensity map. Ground failure probability due to soil liquefaction was also determined, and finally, interpolated maps were created for the research with better accuracy; these maps are crucial to achieving sustainable development goals [23]. Rahman et al. (2023) revealed that GIS can effectively identify the most vulnerable region for soil liquefaction geohazard [24]. Hossain et al. (2022) checked the accuracy of IDW interpolation geohazard maps. The obtained R2 values for each regression analysis event were more than 0.79 [25]. In 2023, Civelekler utilized GIS to develop allowable BC maps for Turkiye. The SPT data from different borelogs was used to assess the BC. Another investigation was conducted in 2022 to visualize the soil properties of Turkiye using GIS [26-27]. Iscan and Guler applied GIS to collect data for soil mapping [28]. Mohtashami et al. developed maps of soil strength properties based on GIS [29]. Numerous researchers employed the IDW interpolation method in creating geotechnical maps, despite the availability of the more advanced technique Kriging. Previous research has indicated that IDW methods are more suitable for mapping soil geotechnical properties. Kriging does not result in more detailed maps compared to IDW, and it also leads to high RMSE for all geotechnical and geophysical properties [30]. According to Ijaz et al. [31], IDW has proven to be very accurate in predicting soil properties using current data.

The purpose of this study is to create IDW interpolation maps for corrected SPT-N values and allowable bearing capacity of soil in Bogura District. The thematic maps will display the changes in soil bearing capacity based on geographic coordinates and depth. In order to meet research goals, geotechnical information, including soil type, N value, and groundwater table depth at various depths, was gathered from 255 investigation reports in Bogura District. The information was then applied to assess adjusted N values using empirically derived equations that can be used universally. A spreadsheet was created to determine the permissible bearing capacity based on adjusted SPT-N values, applying the bearing capacity formulas for depths of 1.5m, 3m, 6m, and 9m beneath the surface. In conclusion, spatial distribution maps were generated for the corrected N value and ABC of soil with the use of geographic coordinates and their respective values. The findings are important for initial planning, desk reviews, hazard recognition, and the preparation of a thorough soil investigation.

2. Study area

2.1. General

The Bogura district can be found in the northwestern region of Bangladesh within the fertile Bengal Delta area. The geomorphology of Bogura city has been formed by natural processes that take place along the Ganges-Brahmaputra-Meghna (GBM) river system. Due to its elevated position relative to the adjacent floodplains, Bogura is situated in the geomorphic area known as the Barind Tract. The landscape in Bogura is fairly level and slightly rolling, with an average height of 30 to 40 meters above sea level. Figure 1 displays the study area map.
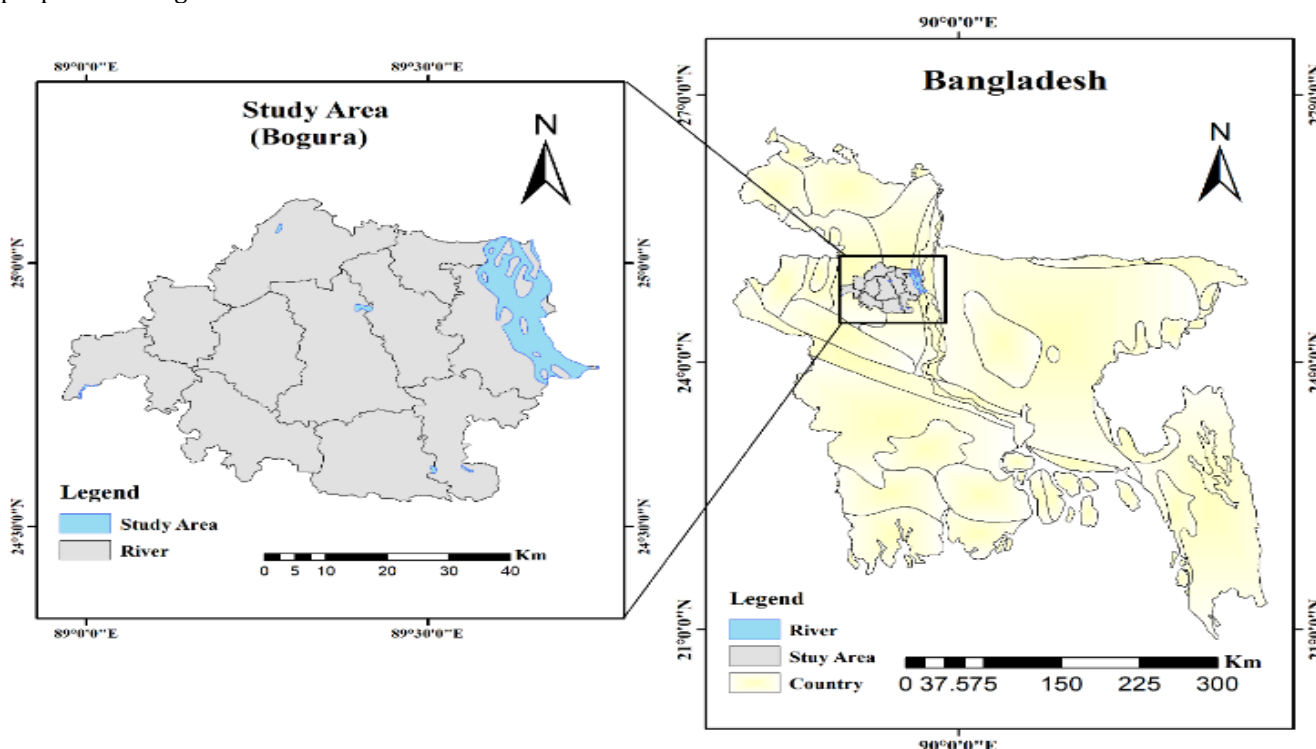

Figure 1. Geographical location of the study area

2.2. Geomorphology

The Food and Agriculture Organization's (FAO) digital soil map, shown in Figure 2, depicts the soil classification in Bogura District. Since sand makes up more than 40% of all soil types, it is evident in Figure 2 that sand is the predominant soil texture. Soil that forms naturally when parent rock material weathers and breaks down—without being moved or deposited—is known as clay residuum [32]. Of the district of Bogura, 44% is covered with this type of soil [23].
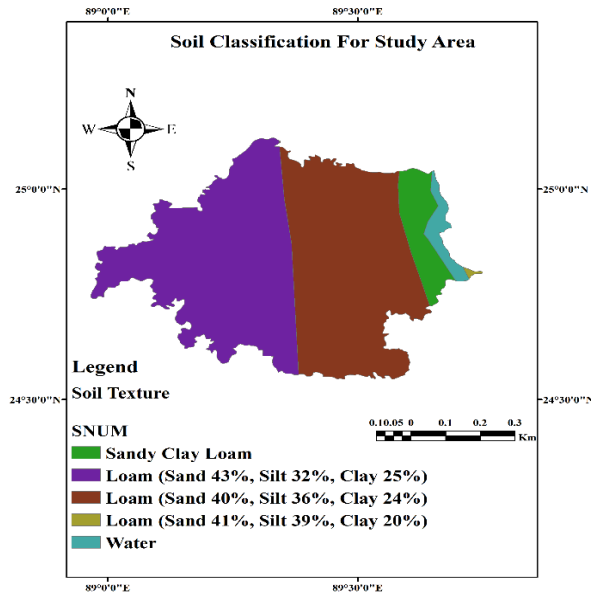

Figure 2. Digital soil texture map for Bogura by FAO

2.3. Hydrological conditions

Groundwater has a significant role in determining bearing capacity. The bearing capacity is lowered at a given depth when the effective confining stress is reduced due to a shallow groundwater level. Data from borehole records was used to analyze the groundwater table. A map of the research region that illustrates the groundwater level is presented in Figure 3. The descriptive statistical assessment of the GWT data is displayed in Table 1.
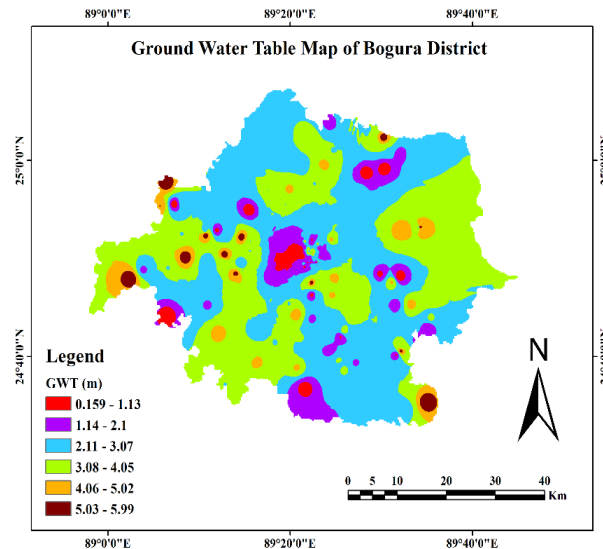

Figure 3. Spatial distribution of depth of GWT

According to a statistical study, the groundwater table in the Bogura area has an average depth of 2.8 meters, with a range of values from 0.15 meters to 6 meters. In this work, ArcGIS was used to investigate groundwater depths. The findings demonstrated that the groundwater in the research region is normally located between 0.15 and 6.0 meters below the surface of the earth. Approximately 84.96% of the drilling locations had a GWT between 2.1 and 4.05 meters, while 10% had a GWT below 2 meters, according to the GWT data analysis.

Table 1. Descriptive statistical analysis of GWT data

Descriptive Statistics	Values	Descriptive Statistics	Values
Mean	2.776	Kurtosis	-0.12
Median	3.05	Skewness	0.20
Standard Deviation	1.43	Minimum	0.15
Sample Variance	2.07	Maximum	6

2.4. Geotechnical conditions

The soil investigation reports that were gathered for this study from several private companies included a range of test outcomes. The test involves drilling a hole at the necessary depth, between 55 and 100 mm in diameter, and inserting a split spoon sampler into the soil. A 63.5 kg hammer is dropped from a height of 750 mm onto a drill rod to accomplish the task. The penetration resistance is defined as the number of strikes N needed to achieve a 300 mm penetration. The blows needed to extend the penetration from 150 mm to 450 mm make up the N-value; the strikes required for the initial 150 mm of penetration are not included to prevent seating mistakes. The field N-value, which has undergone numerous modifications by the standard evaluation method, is utilized to interpret SPT findings [33]. The research region and BHs distribution are displayed in Figure 4. The test results show that the research area's soil was composed of clay down to a depth of 3 meters and that between 3 and 10 meters, the soil type was sand containing little silt.
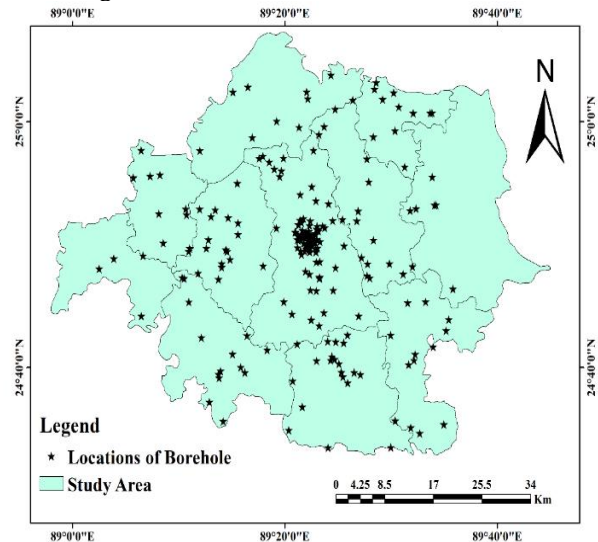

Figure 4. Borehole locations

2.5. Data set

The data set includes SPT-N values obtained from SPT tests performed at various depths (1.5, 3, 6, and 9 m below EGL) as well as the GWT for 255 BH. Only 60 BHs are included in Table 2 due to the significant amount of space needed to display such data.

Table 2. Coordinates, field SPT value and GWT of 60 BHs

BH No.	GPS Coordinates		GWT	SPT			
	Lat.	Long.		1.5 m	3m	6m	9m
1	24.842	89.375	6	7	11	11	24
2	24.731	89.375	1.52	6	9	11	18
3	24.841	89.374	2.8	6	10	16	34
4	24.987	89.506	0.3	7	10	18	9
5	24.842	89.357	0.61	5	14	20	31
6	25.040	89.367	3.5	9	15	11	28
7	24.820	89.359	0.65	4	9	15	40
8	24.771	89.409	4.27	10	15	15	17
9	24.800	89.042	6	6	10	44	50
10	24.860	89.355	0.76	12	14	37	50
11	24.690	89.305	3.05	10	12	43	50
12	24.660	89.422	4.5	14	17	15	23
13	24.827	89.366	0.61	12	10	11	22
14	24.667	89.264	3.66	13	13	24	36
15	24.844	89.355	0.31	2	7	12	24
16	24.852	89.385	1.52	12	7	11	8
17	24.846	89.382	3.05	7	11	9	13
18	24.829	89.353	1.52	10	18	10	30
19	24.887	89.568	2.44	9	18	34	36
20	24.901	89.357	2.44	2	2	4	26
21	24.844	89.375	3.05	10	11	9	24
22	24.833	89.372	0.61	10	11	9	24
23	25.011	89.535	1.22	5	8	14	23
24	24.892	89.382	3.05	12	10	13	33
25	24.842	89.376	4	8	10	16	30
26	24.828	89.373	1.83	5	6	17	41
27	24.842	89.357	0.91	5	6	18	17
28	24.860	89.355	2.13	5	9	13	30
29	25.063	89.406	1.52	2	7	14	22
30	24.844	89.357	1.22	5	10	9	33
31	25.063	89.406	1.52	2	7	14	22
32	24.844	89.357	1.22	5	10	9	33
33	24.660	89.422	2.5	9	12	14	29
34	24.860	89.355	2.13	10	12	18	31
35	24.831	89.376	3	8	10	13	26
36	24.671	89.418	2.44	3	3	11	16
37	24.854	89.384	1.52	5	7	8	10
38	24.558	89.500	3.05	7	4	11	12
39	24.824	89.382	4	10	5	9	35
40	24.710	89.500	3.05	9	19	7	24
41	24.676	89.536	5.7	5	9	4	4
42	24.594	89.507	3.05	12	6	6	8
43	24.787	89.388	4	18	24	12	29
44	24.868	89.363	3	7	10	13	28
45	24.844	89.372	4.7	9	9	6	23
46	24.840	89.213	6	8	8	18	39
47	24.739	89.344	5	22	24	22	37
48	24.841	89.380	2	9	10	7	19
49	24.870	89.244	6	10	15	18	47
50	25.039	89.504	6	9	12	11	25
51	24.828	89.210	3.05	6	8	16	39
52	24.585	89.531	3.05	5	6	9	9
53	24.702	89.401	3.05	5	7	18	31
54	24.979	89.472	0.4	3	4	16	18
55	24.816	89.454	3	2	4	10	30
56	24.793	89.372	6	14	13	9	25
57	24.589	89.583	6	18	21	24	15
58	24.860	89.355	6	7	10	16	25
59	25.031	89.369	3.5	10	15	9	7
60	24.788	89.467	3.5	12	5	8	30

3. Method

3.1. Corrections of SPT-N

The accurate SPT-N value is determined from the field N value using a variety of modifications, such as adjustments for the water table, overburden pressure, and field method. Various studies established empirical correlations to determine the accurate N value. The sections that follow describe the rectification processes.

3.1.1. SPT-N corrections for field procedures

Modifications are done for energy transmission by hammer, sampler size and shape, borehole size, and blow count rate throughout the field method. The height of the fall, the system's efficiency, and the actual weight of the hammer are all taken into consideration by the energy transfer correction factor. The surface area of the sampler and its form factor are taken into consideration by the factor that corrects for sampler size and shape. The discrepancy between the sampler and borehole diameters is included in the adjustment factor for borehole diameter. The following Equation 1 was created by Skempton in 1986 to adjust the field N value for field processes [34].

$$N_{(60)} = (N . C_S . C_B . C_R . E_H)/0.60 \qquad (1)$$

where, $N_{(60)}$ = field procedure correction of N; N = field N value; C_S = sampler correction factor; C_B = correction for bore log diameter; C_R = correction factor for rod length; and E_H = correction factor for efficiency of hammer.

The actual value of C_S in Equation 1 is determined by what kind of sampler is utilized in the conventional penetration test. For a standard sampler, C_S equals 1. In this study, conventional split spoon samplers were employed in the SPT field test. The boring log diameter modification should be introduced when BHs have a diameter of more than 12 cm; in this investigation, the boring log diameter was 10 cm, hence the factor of correction (C_B) was used 1. In the actual field test, a hand-drop Donut hammer was utilized for determining the N value; therefore, the energy adjustment factor was set to 0.6 in this study [11, 34-35]. The coefficient of correction for a rod (C_R) may be set to 0.75 for rod lengths up to 4 m; 0.85 for rod lengths up to 6 m; and 1 for rod lengths higher than 10 m [3].

3.1.2. corrections for overburden pressure

The pressure from the soil's weight affects how difficult it is to push a tool into the ground in sandy soils. This pressure is typically too low when the tool is used close to the surface. However, if the tool is pushed

deeper, the same type of soil with the same compactness will offer more resistance. Gibbs & Holtz suggested in 1957 that adjustments should be made to field test values depending on the depth at which they were taken [36]. Since then, various studies have recommended different correction levels for different depths. Equation 2 can be used to correct field test data and account for the overburden pressure.

$$N_{1(60)} = C_N * N_{(60)} \qquad (2)$$

Where C_N represents correction factor for overburden pressure. Peck et al. [11] discovered the equation that is commonly used for C_N, as seen in Eqn. 3. This relationship was developed in 1974. This equation is also applicable to Bangladesh according to BNBC 2015 [37].

$$C_N = 0.77 \log(\frac{2000}{\sigma'}) \qquad (3)$$

where σ' is the effective stress expressed in kN/m². As the soil strata at 3 m range from silty clay to soft clay, the dry and saturated unit weights are 15 kN/m³ and 17 kN/m³, respectively. Within three to nine meters of the research area, the soil type is sandy. Equations 4 and 5 for sandy soil were used to get the unit weights for both dry and saturated soil [11, 37-38].

$$\gamma_{moist} = 16 + 0.1 * N_{(60)} \qquad (4)$$
$$\gamma_{submerged} = 8.8 + 0.01 * N_{(60)} \qquad (5)$$

3.1.3. SPT-N corrections for GWT

When there is fine sand or silt below the water table, the investigators recommended correcting the SPT value for the water table. It appears that the dilatancy effect can cause large N-values, particularly when the measured value is more than 15. The soil's resistance and, consequently, the N value are influenced by the pore pressure. In such circumstances, Terzaghi and Peck (1996) propose applying the following Equation 6 [39].

$$N_{1(60)COR} = 15 + \frac{1}{2}\left(N_{1(60)} - 15\right) \text{ for } N_{1(60)} > 15 \quad (6)$$

$N_{1(60)COR}$ = Correction of SPT-N for the GWT [34, 40].

3.2. Bearing capacity of soil

The allowed BC of the soil was calculated using the results of SPTs performed at various depths for each borehole. The soil's BC can be computed using the adjusted N values. A high safety factor of three is used to calculate the soil's permitted bearing capacity because of the soil's heterogeneity, high GWT, and organic matter. Using a safety factor of three, the ultimate BC of the soil is determined using the following equations 7 through 12 [41-42].

$$q_{ult.net} = \frac{N_{1(60)cor}}{0.08}\left(\frac{B+0.3}{B}\right)^2 F_d\left(\frac{S_e}{25}\right) \qquad (7)$$

The following equation (8) can potentially be estimated for a wide-raft foundation:

$$q_{ult} = \frac{N_{1(60)cor}}{0.08} F_d\left(\frac{S_e}{25}\right) \qquad (8)$$

$$F_d = 1 + 0.33\left(\frac{D_f}{B}\right) \leq 1.33 \qquad (9)$$

where: $q_{ult.net}$ = net ultimate soil BC (kN/m²); B = width of footings (m); S_e= settlement of soil = 25 mm (assumed) [43]; D_f/B ratio is equal to unity (assumed).

The following equations can be used to calculate the allowable bearing capacity of soil.

$$q_{all} = q_{all.net} + \gamma'D_f \qquad (10)$$
$$q_{all.net} = \frac{q_{ult,net}}{FS} \qquad (11)$$
$$q_{all} = \frac{q_{ult,net}}{FS} + \gamma'D_f \qquad (12)$$

In the above equations, q_{all} = allowable soil BC; $q_{all.net}$ = net allowable soil BC; γ' = effective unit weight; D_f = footing depth from ground surface; and FS = safety factor = 3 (assumed).

4. Results and discussion

4.1. Allowable bearing capacity

The ultimate bearing capacity at various depths was determined using the vast quantity of data collected from 255 BHs over the whole research region. Table 3 only displays a calculated allowable soil-bearing capacity based on raft footing for 60 boreholes. Table 4 displays the descriptive statistics for the corrected N value and permissible soil load bearing capacity of all the data.

Statistical analysis of the research outcomes shows the minmax value of the corrected N value and allowable bearing capacity for 255 BHs. The minimum and maximum values of corrected N for 1.5 m depth are 1.13 and 24.76, respectively. For depth 3 m, it is 1.9 and 22.84; for depth 6 m, it is 2.66 and 31.79; and for depth 9 m, it is 3.55 and 34.34. The mean allowable bearing capacity for depths 1.5, 3, 6, and 9 m is 58.24 kN/m², 76.28 kN/m², 130.84 kN/m², and 189.27 kN/m², respectively.

4.2. SPT-N modeling

After analyzing data gathered from 255 BH SPTs, GIS was utilized to generate a thematic map depicting the variation in the adjusted SPT-N number at different depths in this study region. Figures 5-8 depict interpolation maps with adjusted SPT-N value fluctuations to a depth of 9 meters.
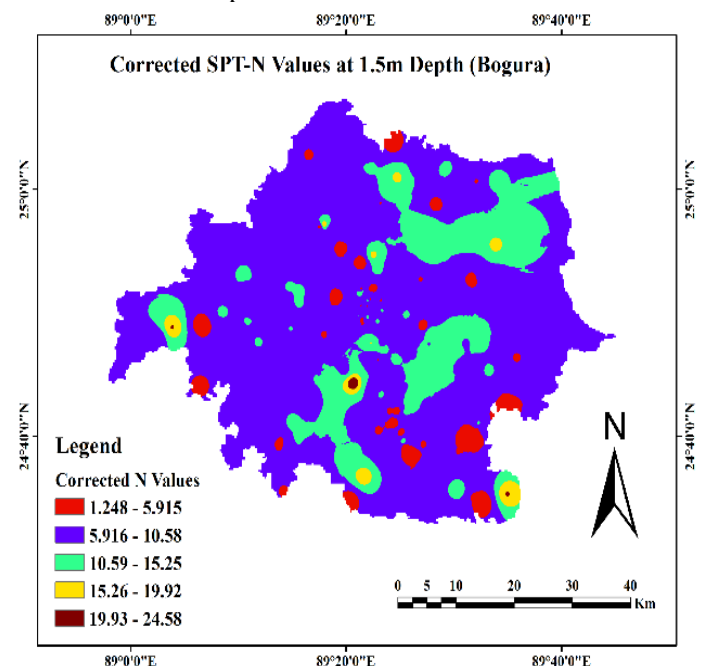

Figure 5. Thematic map depicts the variance of corrected SPT-N values at depth of 1.5 m

Table 3. Allowable BC of Bogura soil assessed from adjusted SPT-N value for 30 BHs

BH	1.5m		3m		6m		9m	
	$N_{1(60)cor}$	q_{all} (kN/m²)	$N_{1(60)cor}$	q_{all} (kN/m²)	$N_{1(60)cor}$	q_{all} (kN/m²)	$N_{1(60)cor}$	q_{all} (kN/m²)
1	7.88	54.44	10.47	79.59	9.32	105.01	17.73	179.51
2	6.75	48.21	9.23	72.72	10.69	112.60	16.24	170.74
3	6.75	48.21	9.60	74.77	14.80	135.63	23.14	210.34
4	8.82	59.69	11.10	83.08	16.63	145.88	9.12	130.51
5	6.09	44.54	15.10	105.25	17.51	150.85	22.89	208.70
6	10.13	66.92	14.27	100.65	10.01	108.83	20.20	193.54
7	4.85	37.68	9.75	75.60	15.01	136.75	27.24	233.58
8	11.25	73.15	14.27	100.65	13.26	127.05	15.15	164.61
9	6.75	48.21	9.52	74.33	25.18	194.58	27.95	238.36
10	14.40	90.58	15.03	104.86	25.74	197.33	31.94	260.48
11	11.25	73.15	11.42	84.86	26.66	202.73	29.95	249.45
12	15.76	98.10	15.59	107.96	13.17	126.55	17.71	179.31
13	14.62	91.79	10.86	81.75	11.06	114.65	18.47	183.44
14	14.63	91.86	12.37	90.12	18.19	154.83	23.59	213.01
15	2.52	24.74	7.77	64.63	12.20	121.02	19.58	189.76
16	13.51	85.63	7.18	61.36	10.69	112.60	7.83	123.28
17	7.88	54.44	10.47	79.59	8.32	99.37	12.14	147.59
18	11.25	73.15	16.73	114.28	9.72	107.18	21.94	203.35
19	10.13	66.92	16.30	111.90	23.15	182.82	24.22	216.50
20	2.25	23.26	1.95	32.38	3.79	74.01	19.69	190.54
21	11.25	73.15	10.47	79.59	8.32	99.37	18.58	184.22
22	12.18	78.29	11.95	87.79	9.05	103.41	19.46	189.09
23	5.63	41.97	8.35	67.84	13.72	129.55	18.74	185.02
24	13.51	85.63	9.52	74.33	11.97	119.80	22.58	207.15
25	9.00	60.68	9.52	74.33	14.24	132.53	20.87	197.42
26	5.63	41.97	6.05	55.10	15.63	140.28	26.86	231.55
27	5.91	43.56	6.39	56.98	16.41	144.66	15.92	168.88
28	5.63	41.97	8.93	71.06	12.34	121.85	21.65	201.74
29	2.25	23.26	7.18	61.36	13.57	128.71	18.15	181.66
30	5.63	41.97	10.44	79.43	8.85	102.30	23.51	212.31

Table 4. Descriptive statistics of allowable BC and Corrected SPT-N of Bogura soil for 255 BHs

| Statistics	1.5m		3m		6m		9m	
	$N_{1(60)corr}$	q_{all}	$N_{1(60)corr}$	q_{all}	$N_{1(60)corr}$	q_{all}	$N_{1(60)corr}$	q_{all}
Mean	8.56	58.24	9.87	76.28	13.93	130.84	19.45	189.27
Median	7.88	54.44	9.52	74.33	13.75	129.74	19.58	189.80
Standard Deviation	3.89	21.56	3.72	20.62	5.16	28.99	5.58	31.82
Kurtosis	1.20	1.20	0.55	0.55	0.08	0.10	0.35	0.32
Skewness	0.75	0.75	0.36	0.36	0.41	0.43	-0.29	-0.27
Range	23.63	130.98	20.94	116.04	29.13	163.72	30.79	174.90
Minimum	1.13	17.02	1.90	32.10	2.66	67.69	3.55	99.21
Maximum	24.76	148.00	22.84	148.14	31.79	231.42	34.34	274.12
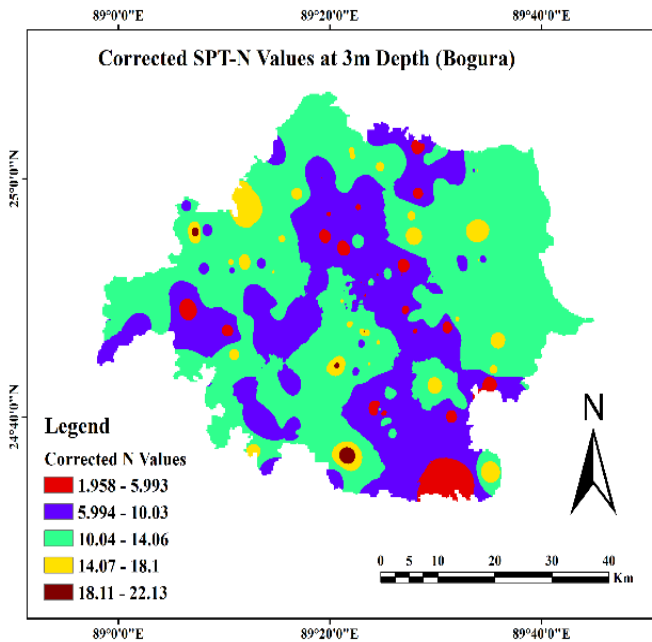
Figure 6. Thematic map depicts the variance of corrected SPT-N values at depth of 3 m

The IDW interpolation technique was used to generate corrected SPT-N value mappings for the research region, with a beginning point of 1.5 m and an ending point of 9 m derived from SPT reports. A map developed to illustrate the simultaneous variance in soil composition throughout layers is presented in Figure 5. The map indicates that the SPT characteristic of the western province is higher in Bogura soils. In comparison, the map displays a minimum value of 1.25 and the greatest value of 24.58 at the level of (0-1.5) m. Figure 6 depicts the maximum value of 22.13 and its smallest value of 1.95 in the IDW technique at a depth of (1.5-3) m.
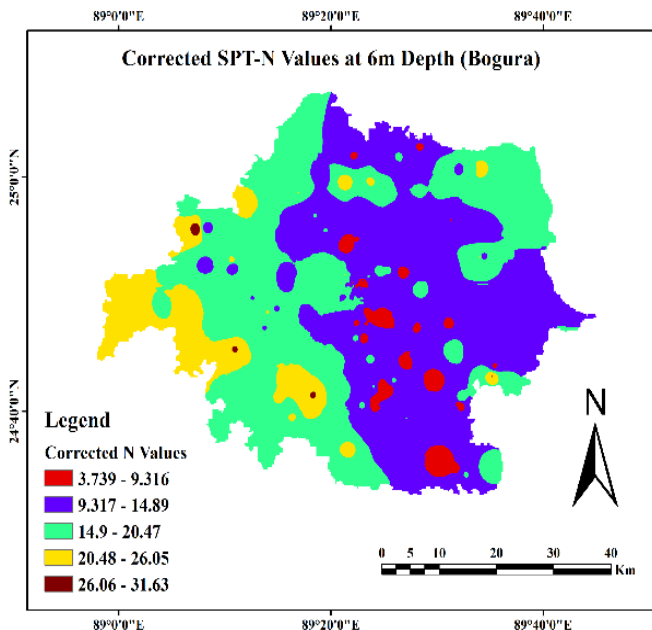
Figure 7. Thematic map depicts the variance of corrected SPT-N values at depth of 6 m

According to Figure 7, the western regions at a depth of (3-6) m have the maximum value of 31.63, while the southern regions have the lowest value of 3.74. In Figure

8, the lowest value (3.83) and the greatest value (34.28) occur at a depth of (6–9) m. The standard penetration test values are displayed in the geotechnical study result at 1.5 meters below the surface, indicating that the soil in these locations is soft and does not tolerate well. The number of blows rises with depth from the soil's surface layer, creating the illusion that the soil is stronger than the layer above it and can support heavier loads. The map displays several blows that vary from 3.7 to 31.63 per borehole.
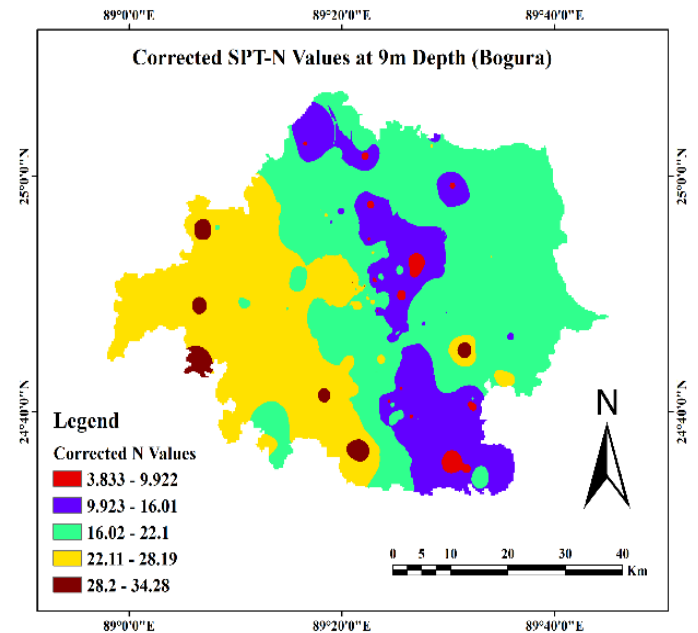

Figure 8. Thematic map depicts the variance of corrected SPT-N values at depth of 9 m

This indicates that the soil in the area, specifically at a depth of 3 to 6 meters, is firm and has a significant load-bearing capacity. However, the map also reveals that the total amount of blows at a depth of 6 to 9 meters exceeds 31.63, suggesting that the soil in this layer has become stiffer than the layer before.

4.3. Bearing capacity modeling

GIS was utilized to analyze data from soil investigations at 255 sites in the research area to create thematic maps showing the variability in allowable bearing capacity of shallow foundations at various depths. It is crucial to refrain from utilizing any extreme SPT values when determining the permissible bearing capacity of shallow foundations with GIS due to the considerable variation and possible outliers in the results of SPTs carried out at various depths in 255 bore-logs. The variability in extremes may result from only a few BHs being drilled in specific parts of the study area or a significant variation in the geotechnical characteristics of soil in certain areas of the study area.

The IDW interpolation approach was utilized to develop the soil bearing capacity maps, as it is thought to be the most effective way to generate the final map of permissible bearing capacity that can be utilized for conceptual engineering design [41]. The theme maps for the variance in soil carrying capacity at 1.5, 3, 6, and 9 m for 255 bore logs are shown in Figures 9 to 12.
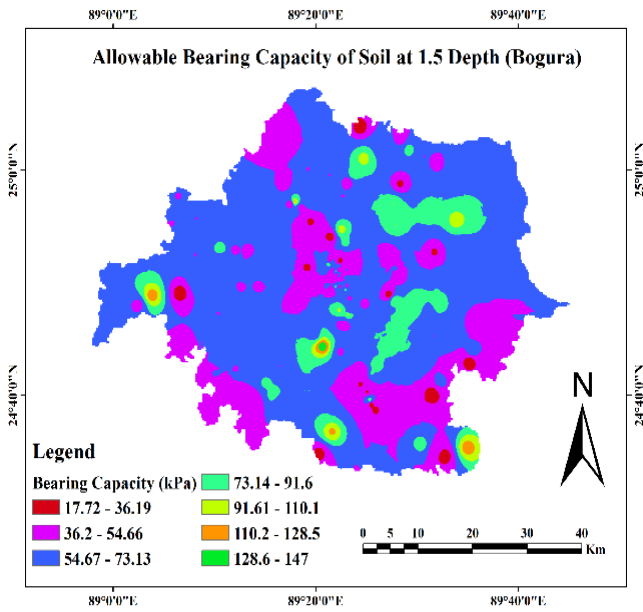
Figure 9. Thematic map indicating the variance in allowable BC of shallow footing (1.5 m)
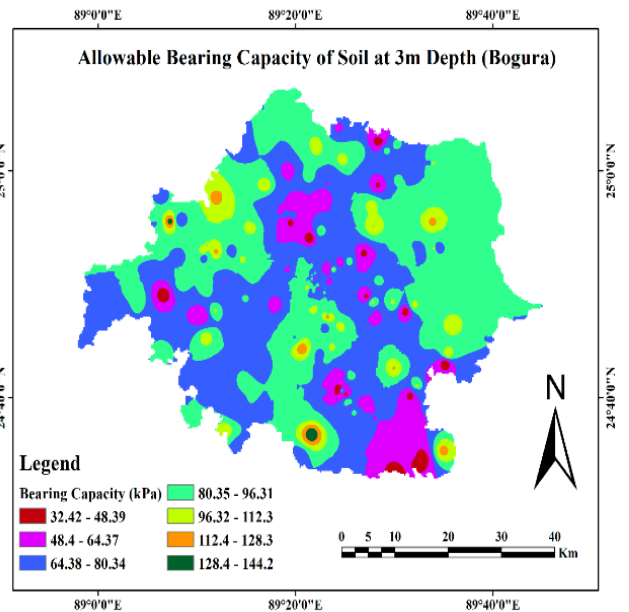

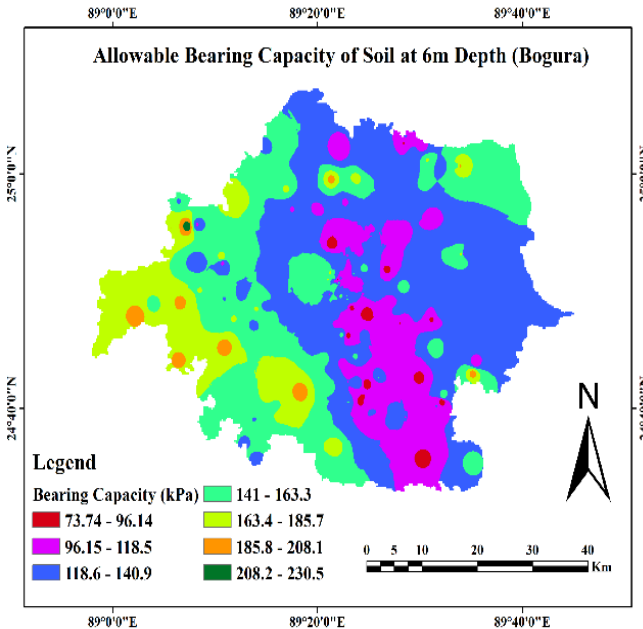**Figure 10.** Thematic map indicating the variance in allowable BC of shallow footing (3 m)

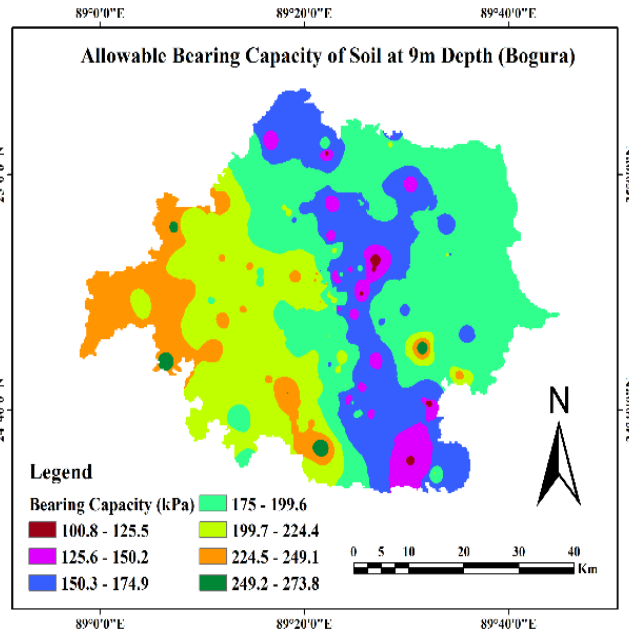**Figure 11.** Thematic map indicating the variance in allowable BC of shallow footing (6 m)

Figure 12. Thematic map indicating the variance in allowable BC of shallow footing (9 m)

The IDW method-created interpolation map indicates that the soil bearing capacity ranges from 17.72 to 147 kN/m² at a depth of 1.5 m (Figure 9). The study area is mostly covered by the color blue, with bearing capacity ranging from 54.67 to 73.13 kN/m². Figure 10 shows a decline in the blue hue and a rise in the spring green, signaling a growth in bearing capacity. Capacity ranges from 32.42 kN/m² to 144.2 kN/m² at a 3 m depth. The capacity range in Bogura city center from south to north is between 96.15 and 118.5 kN/m² (Figure 11). The spring green color in the western area of the study region shows a bearing capacity ranging from 141 to 163.3 kN/m². Nonetheless, the weakest bearing capacity can be found in certain regions extending from the southern to central parts of Bogura.

Remarkably, the soil load-carrying capacity increased in certain lime green and orange sections in the

west of the Bogura district, where it ranged from 224.5 to 249.1 kN/m² at level 9 m (Figure 12). In addition to providing important background information for the research region, this empathetic map facilitates a visual understanding of the data. Additionally, adopting these maps into practice will result in lower costs in addition to time and effort. Making thematic maps with soil geotechnical data has the additional advantage of helping authorities and designers select the best option for any construction design, the most suitable foundation construction, and the necessary soil treatment.

5. Conclusion

The following conclusions may be drawn from the outcomes of this research:
❖ Data from borehole logs were gathered from 255 points throughout Bogura District, Bangladesh. Maps

based on GIS were also made to display the locations of the gathered bore logs around the city.

❖ By utilizing a spreadsheet, inputting data such as soil type, GWT location from ground surface, and SPT-N value at 1.5m depth. Calculations were made for boreholes that were collected at 3m, 6m, and 9m depths. Using the same spreadsheet, an estimate was made for the corrected N value and the allowable BC of soil for the entire study area.

❖ The IDW interpolation maps of adjusted N values and the permissible soil-bearing capacities at specified depths were also constructed and examined.

❖ Utilizing the adjusted N values, geohazards such as soil liquefaction and ground failure probability may be recognized and mitigated for various soil layers, resulting in more durable constructions.

❖ Using GIS-generated thematic maps to determine soil load-bearing capacity can save time and funds, particularly for small construction projects.

❖ Local government agencies can utilize these maps to obtain direct information on the bearing capacity.

❖ Maps of soil bearing capacity and corrected N values may also be beneficially used for various shallow and deep foundation design types.

❖ These maps may be used to evaluate the foundations of both newly constructed and asymmetrically designed structures, as well as to determine the degree of failure and collapse danger.

Author contributions

Md. Mahabub Rahman: Conceptualization, Data collection, Methodology, Data curation, Software, Validation, Visualization, Writing-Original draft, Writing-Reviewing and Editing.

Conflicts of interest

The authors declare no conflicts of interest.

References

1. Lowe, J., & Zaccheo, P. F. (1991). Subsurface explorations and sampling. Foundation engineering handbook, 1-71. https://doi.org/10.1007/978-1-4757-5271-7_1

2. Hassan, W., Raza, M. F., Alshameri, B., Shahzad, A., Khalid, M. H., & Nawaz, M. N. (2023). Statistical interpolation and spatial mapping of geotechnical soil parameters of District Sargodha, Pakistan. Bulletin of Engineering Geology and the Environment, 82(1),37. https://doi.org/10.1007/s10064-022-03059-2

3. Rahman, M. M. (2019). Foundation design using standard penetration test (spt) n-value. Researchgate,5,1-39. https://doi.org/10.13140/RG.2.2.23159.73123

4. ASTM. (1999). ASTM D1586-99 standard test method for penetration test and split-barrel sampling on soils. Annual Book of ASTM Standards, American Society of

5. AASHTO. (2009). AASHTO T-206 method of test for penetration test and split-barrel sampling of soils.

6. Rocha, B. P., & Giacheti, H. L. (2018). Site characterization of a tropical soil by in situ tests. Dyna,85(206),211-219. https://doi.org/10.15446/dyna.v 85n206. 67891

7. Decourt, L. (1990). The Standard Penetration Test, State of the Art Report.(pp. 1-12). Oslo, Norway: Norwegian Geotechnical Institute Publication.

8. Page, M., Bradshaw, A. S., & Mike Sherrill, P. E. (2005). Guidelines for Geotechnical Site Investigations in Rhode Island Final Report. University of Rhode Island: Narragansett, RI, USA.

9. Ghafghazi, M., DeJong, J. T., Sturm, A. P., & Temple, C. E. (2017). Instrumented Becker penetration test. II: iBPT-SPT correlation for characterization and liquefaction assessment of gravelly soils. Journal of Geotechnical and Geoenvironmental Engineering, 143(9),04017063. https://doi.org/10.1061/(ASCE)GT.1943-5606.0001718

10. Bahmani, S. M., & Briaud, J. L. (2020). Modulus to SPT blow count correlation for settlement of footings on sand. In Geo-Congress 2020 (pp. 343-349). Reston, VA: American Society of Civil Engineers. https://doi.org/10.1061/9780784482780.033

11. Peck, R. B., Hanson, W. E., & Thornburn, T. H. (1991). Foundation engineering. John Wiley & Sons.

12. Craig, R.F. (2004). Soil Mechanics. Spon, Taylor & Francis Group: New York, NY, USA.

13. Matsumoto, T., Phan, L. T., Oshima, A., & Shimono, S. (2015). Measurements of driving energy in SPT and various dynamic cone penetration tests. Soils and Foundations,55(1),201-212. https://doi.org/10.1016/j.sandf.2014.12.016

14. Habib, W., Mahmood, S., Noor, S., Saleem, A., Siraj, M., & Ahmad, H. (2023). A post earthquake damage assessment using GIS in district Mirpur, Pakistan. Advanced GIS, 3(2), 53-58.

15. Onyıl, H. I. (2022). Geospatial intelligence (GeoINT) risk maps producing with geographic information systems (GIS) and creation of the 2D simulation model. Advanced GIS, 2(1), 01-07.

16. Cabalar, A. F., Karabas, B., Mahmutluoglu, B., & Yildiz, O. (2021). An IDW-based GIS application for assessment of geotechnical characterization in Erzincan, Turkey. Arabian Journal of Geosciences, 14(20), 2129. https://doi.org/10.1007/s12517-021-08481-6

17. Al-Maliki, L. A. J., Al-Mamoori, S. K., El-Tawel, K., Hussain, H. M., Al-Ansari, N., & Al Ali, M. J. (2018). Bearing capacity map for An-Najaf and Kufa cities using GIS. Engineering, 10(05), 262. https://doi.org/10.4236/eng.2018.105018

18. Yakar, M., Yilmaz, H. M. & Mutluoglu, O. (2010). Close range photogrammetry and robotic total station in volume calculation. International Journal of the Physical Sciences. 5(2), 086-096

19. Adesina, E., Ajayi, O., Odumosu, J., & Illah, A. (2024). Assessing the risk of soil loss using geographical

information system (GIS) and the revised universal soil loss equation (RUSLE). Advanced GIS, 4(2), 42-53.

20. Yakar, M., & Dogan, Y. (2019). 3D Reconstruction of Residential Areas with SfM Photogrammetry. In Advances in Remote Sensing and Geo Informatics Applications: Proceedings of the 1st Springer Conference of the Arabian Journal of Geosciences (CAJG-1), Tunisia 2018 (pp. 73-75). Springer International Publishing. -45.

21. Unel, F. B., Kusak, L., & Yakar, M. (2023). GeoValueIndex map of public property assets generating via Analytic Hierarchy Process and Geographic Information System for Mass Appraisal: GeoValueIndex. Aestimum, 82, 51-69..

22. Topaloglu, R. H. (2022). Investigation of Land Use/Land Cover change in Mersin using geographical object-based image analysis (GEOBIA). Advanced Remote Sensing, 2(2), 40–46.

23. Hossain, M. B., & Rahman, M. (2025). Seismic microzonation and probability of ground failure assessment caused by liquefaction for Bogura District, Bangladesh, Journal of Rehabilitation in Civil Engineering,13(2),222-247. https://doi.org/10.22075/jrce.2024.34111.2086

24. Rahman, M. M., Hossain, M. B., & Roknuzzaman, M. (2023). Effect of peak ground acceleration (PGA) on liquefaction behavior of subsoil: A case study of Dinajpur Sadar Upazila, Bangladesh. In AIP Conference Proceedings, 2713(1),1-13. https://doi.org/10.1063/5.0129770

25. Hossain, M. B., Roknuzzaman, M., & Rahman, M. M. (2022). Liquefaction Potential Evaluation by Deterministic and Probabilistic Approaches. Civil Engineering Journal, 8(7), 1459-1481. https://doi.org/10.28991/CEJ-2022-08-07-010

26. Civelekler, E. (2023). Using GIS for the allowable soil bearing capacity estimation according to the Terzaghi (1943) equation in Eskişehir city center, Türkiye. International Journal of Engineering and Geosciences, 8(3),310-317. https://doi.org/10.26833/ijeg.1212584

27. Civelekler, E., & Pekkan, E. (2022). The application of GIS in visualization of geotechnical data (SPT-Soil Properties): a case study in Eskisehir-Tepebaşı, Turkey. International Journal of Engineering and Geosciences,7(3),302-313. https://doi.org/10.26833/ijeg.980611

28. İşcan, F., & Güler, E. (2021). Developing a mobile GIS application related to the collection of land data in soil mapping studies. International Journal of Engineering and Geosciences, 6(1), 27-39. https://doi.org/10.26833/ijeg.677958

29. Mohtashami, S., Hansson, L., & Eliasson, L. (2023). Estimating Soil Strength Using GIS-Based Maps - A case study in Sweden. European Journal of Forest Engineering,9(2),70-79. https://doi.org/10.33904/ejfe.1321075

30. Daniyal, M., Sohail, G. M., & Rashid, H. M. A. (2023). GIS-based mapping of geotechnical and geophysical properties of Lahore soils. Environmental Earth Sciences,82(22),540. https://doi.org/10.1007/s12665-023-11201-w

31. Ijaz, Z., Zhao, C., Ijaz, N., Rehman, Z. U., & Ijaz, A. (2021). Spatial mapping of geotechnical soil properties at multiple depths in Sialkot region, Pakistan. Environmental Earth Sciences, 80(24), 787. https://doi.org/10.1007/s12665-021-10084-z

32. FAO. (1995). Digital soil map of the world and derived soil properties. Food and Agriculture Organization.

33. Youd, T. L., & Idriss, I. M. (2001). Liquefaction resistance of soils: summary report from the 1996 NCEER and 1998 NCEER/NSF workshops on evaluation of liquefaction resistance of soils. Journal of geotechnical and geoenvironmental engineering, 127(4),297-313. https://doi.org/10.1061/(ASCE)1090-0241(2001) 127:4(297)

34. Skempton, A. W. (1986). Standard penetration test procedures and the effects in sands of overburden pressure, relative density, particle size, ageing and overconsolidation. Geotechnique, 36(3), 425-447. https://doi.org/10.1680/geot.1986.36.3.425

35. Bolton Seed, H., Tokimatsu, K., Harder, L. F., & Chung, R. M. (1985). Influence of SPT procedures in soil liquefaction resistance evaluations. Journal of geotechnical engineering, 111(12), 1425-1445. https://doi.org/10.1061/(ASCE)07339410(1985)11 1:12(1425)

36. Gibbs, H. (1957). Research on determining the density of sands by spoon penetration testing. 4th International Conference on SMFE, 35–39.

37. BNBC. (2015). Bangladesh National Building Code.

38. Bowles, J. (1998). Foundation Analysis and Design. McGraw-Hill: New York, NY, USA.

39. Terzaghi, K., Peck, R.B., Mesri, G. (1996). Soil Mechanics in Engineering Practice. Third edit. John Wiley & Sons, New York.

40. Fletcher, G. F. (1965). Standard penetration test: its uses and abuses. Journal of the Soil Mechanics and Foundations Division, 91(4), 67-75. https://doi.org/10.1061/JSFEAQ.0000776

41. Das, B.M. (2015). Principles of Foundation Engineering. Cengage Learning: Boston, MA, USA.

42. Bowles, J. E. (1987). Elastic foundation settlements on sand deposits. Journal of Geotechnical Engineering, 113(8),846-860. https://doi.org/10.1061/(ASCE)07339410(1987)11 3: 8(846)

43. Al-Mamoori, S. K., Al-Maliki, L. A., Al-Sulttani, A. H., El-Tawil, K., & Al-Ansari, N. (2021). Statistical analysis of the best GIS interpolation method for bearing capacity estimation in An-Najaf City, Iraq. Environmental Earth Sciences, 80(20), 683. https://doi.org/10.1007/s12665-021-09971-2